PEDS Advance Access published September 26, 2016

Protein Engineering, Design & Selection, 2016, pp. 1–11
doi: 10.1093/protein/gzw049
Original Article

Original Article

Engineering a minimal G protein to facilitate crystallisation of G protein-coupled receptors in their active conformation

Byron Carpenter* **and Christopher G. Tate***

MRC Laboratory of Molecular Biology, Cambridge Biomedical Campus, Francis Crick Avenue, Cambridge CB2 0QH, UK

*To whom correspondence should be addressed. E-mail: byronc@mrc-lmb.cam.ac.uk (B.C.); cgt@mrc-lmb.cam.ac.uk (C.G.T.)
B.C. conceived the idea, designed the research, and performed all experiments. B.C. and C.G.T. analysed the data and wrote the article.
Edited by: Adrian Goldman

Received 22 April 2016; Revised 1 August 2016; Accepted 23 August 2016

Abstract

G protein-coupled receptors (GPCRs) modulate cytoplasmic signalling in response to extracellular stimuli, and are important therapeutic targets in a wide range of diseases. Structure determination of GPCRs in all activation states is important to elucidate the precise mechanism of signal transduction and to facilitate optimal drug design. However, due to their inherent instability, crystallisation of GPCRs in complex with cytoplasmic signalling proteins, such as heterotrimeric G proteins and β-arrestins, has proved challenging. Here, we describe the design of a minimal G protein, mini-G_s, which is composed solely of the GTPase domain from the adenylate cyclase stimulating G protein G_s. Mini-G_s is a small, soluble protein, which efficiently couples GPCRs in the absence of Gβγ subunits. We engineered mini-G_s, using rational design mutagenesis, to form a stable complex with detergent-solubilised β_1-adrenergic receptor (β_1AR). Mini G proteins induce similar pharmacological and structural changes in GPCRs as heterotrimeric G proteins, but eliminate many of the problems associated with crystallisation of these complexes, specifically their large size, conformational dynamics and instability in detergent. They are therefore novel tools, which will facilitate the biochemical and structural characterisation of GPCRs in their active conformation.

Key words: complex, G protein, G protein-coupled receptor, GPCR, G_s, mini G protein, mini-G_s

Introduction

G protein-coupled receptors (GPCRs) modulate cytoplasmic signalling, through heterotrimeric G proteins and β-arrestins, in response to extracellular stimuli, such as hormones and neurotransmitters (Rosenbaum *et al.*, 2009). The central role of GPCRs in regulating cellular responses makes them an important therapeutic target (Lagerstrom and Schioth, 2008). GPCRs adopt different conformational states in response to binding different classes of ligand and coupling to cytoplasmic signalling proteins. Therefore, structure determination of GPCRs in all activation states is important to decipher the molecular mechanisms of signal transduction, and to facilitate optimal drug design.

Heterotrimeric G proteins are composed of α, β and γ subunits. Gα consists of a GTPase domain (GαGTPase), which is analogous to members of the small GTPase superfamily of proteins, and an α-helical domain (GαAH), which is unique to heterotrimeric G proteins (Sprang, 1997). In the inactive, GDP-bound state, Gα binds Gβγ, forming a heterotrimer with low basal nucleotide exchange activity (Higashijima *et al.*, 1987). The trimer is anchored to the cell membrane, through lipid modifications of both Gα and Gγ (Spiegel

et al., 1991). GPCRs catalyse rapid nucleotide exchange on heterotrimeric G proteins, but only weakly activate the isolated α subunit (Herrmann *et al.*, 2006; Phillips *et al.*, 1992).

Agonist binding to a GPCR promotes its transition to a structural state that can efficiently interact with heterotrimeric G proteins (Lebon *et al.*, 2011b; Rasmussen *et al.*, 2011b; Rosenbaum *et al.*, 2011; Xu *et al.*, 2011). The agonist-bound receptor engages the C-terminal region of Gα (Hamm *et al.*, 1988), initiating a rotation and displacement of the α5 helix (Oldham *et al.*, 2006). This ultimately destabilises the nucleotide-binding pocket and the GαGTPase–GαAH domain interface, allowing GDP to dissociate (Alexander *et al.*, 2014; Dror *et al.*, 2015; Flock *et al.*, 2015; Kaya *et al.*, 2014; Sun *et al.*, 2015; Van Eps *et al.*, 2011). The resulting nucleotide-free ternary complex displays large, mutually induced structural changes in both the receptor and G protein (Rasmussen, *et al.*, 2011b), and is often characterised by increased agonist binding affinity of the receptor (Delean *et al.*, 1980). This complex can be trapped in the absence of guanine nucleotides (Bornancin *et al.*, 1989), but is extremely short-lived *in vivo* due to rapid binding of GTP to Gα (Vuong *et al.*, 1984). GTP binding triggers dissociation of the G protein from the receptor (Kuhn, 1981) and separation of Gα from Gβγ (Fung *et al.*, 1981).

GPCR–G protein complexes are difficult targets for structural studies due to their large size, conformational dynamics, and instability in detergent. To date, only a single structure of a GPCR–G protein complex has been reported, namely the β_2-adrenergic receptor (β_2AR) bound to the adenylate cyclase stimulating G protein G_s (Rasmussen *et al.*, 2011b). This structure provided the first atomic resolution insight into the organisation of the ternary complex, but further structures are required to fully decipher the molecular mechanisms of signal transduction and the specificity for G protein coupling. Given the difficulties in crystallising GPCR–G protein complexes, novel tools are needed to facilitate their high-throughput crystallisation.

Here, we report the design of a minimal G protein, termed mini-G_s, which is composed solely of the GαGTPase domain from G_s. Mini-G_s closely mimics the pharmacological and structural changes induced in GPCRs by heterotrimeric G_s. It is therefore a novel tool, which will facilitate the characterisation of GPCRs in their active conformation, and has allowed the structure determination of the adenosine A_{2A} receptor in the fully active state (Carpenter *et al.*, 2016).

Materials and Methods

Cloning

Details of G protein, β_1AR and mini-G_s constructs used in this work are provided in Supplementary Tables SI–SIII, respectively. All G proteins used in this study were mutated to remove sites of lipid modification. G protein cDNAs were cloned into the transfer vector pBacPAK8 (Clontech), and baculoviruses were prepared using the flashBAC ULTRA system (Oxford Expression Technologies). Synthetic genes (Integrated DNA Technologies) for Nb80 (Rasmussen *et al.*, 2011a) and Nb35 (Westfield *et al.*, 2011) were cloned into pET26b (Novagen) for periplasmic expression in *Escherichia coli*. Mini-G_s constructs, which were derived from the long isoform of the human $G\alpha_s$ gene, were cloned into the pET15b vector (Novagen) for expression in *E. coli*.

Expression and purification of β_1AR

β_1AR constructs were expressed in insect cells using the baculovirus expression system, and purified as described previously (Warne *et al.*, 2003; Warne *et al.*, 2011; Warne *et al.*, 2009).

Baculovirus expression of G proteins

Trichoplusia ni cells (Expression Systems) were grown in ESF921 serum-free media (Expression Systems) in 5 L optimum growth flasks (Thompson Instrument Company). Immediately before infection, heat-inactivated foetal bovine serum (Sigma) was added to a final concentration of 5%. Cells were infected with third passage virus at a final concentration of 3%. In the case of co-infection with multiple viruses (for heterotrimeric G_s or Gβγ) each virus was added to a final concentration of 3%. The final volume of culture was 3 L per flask and the final cell density was 3×10^6 cells/ml. Cells were harvested 48 h post-infection by centrifugation at 5000 *g* for 5 mins, flash-frozen in liquid nitrogen and stored at −80°C.

Protein purification

Details of G protein, nanobody and mini-G_s purifications are provided in the Supplementary material.

Saturation binding assay

Insect cell membranes containing β_1AR were resuspended in assay buffer (20 mM HEPES pH 7.5, 100 mM NaCl). The sample was aliquoted and [^{3}H]-dihydroalprenolol was added (to give final concentrations in the range of 0.25 nM to 256 nM), alprenolol was added to the negative control (1 mM final concentration). Samples were incubated at 20°C for 2 h, before filtering through 96-well glass fibre filter plates (Merck Millipore) and washing with ice-cold assay buffer. Radioactivity was quantified by scintillation counting and apparent K_d values were determined using GraphPad Prism version 5.0 (GraphPad Software, San Diego, CA).

Competition binding assay

Insect cell membranes containing β_1AR were resuspended in assay buffer (25 mM HEPES pH 7.5, 100 mM NaCl, 1 mM $MgCl_2$, 1 mM ascorbate). The sample was aliquoted and binding partner (25 μM final concentration), isoprenaline (final concentrations in the range of 1 pM–100 mM) and apyrase (0.1 U/ml final concentration) were added. Alprenolol was added to the negative control (100 μM final concentration). Samples were incubated at 20°C for 1.5 h, before adding [^{3}H]-dihydroalprenolol (5 or 20 nM final concentrations for $\beta_1AR^{\Delta NC}$ or β_1AR-84, respectively). Samples were incubated at 20°C for 1.5 h, before filtering through 96-well glass fibre filter plates and washing with ice-cold assay buffer. Radioactivity was quantified by scintillation counting and K_i values were determined using GraphPad Prism version 5.0.

Competition binding assays using detergent-solubilised β_1AR-84 were performed using a similar protocol, except: all steps were performed at 4°C; membranes were solubilised with dodecyl maltoside (DDM; 0.1% final concentration) for 30 min, prior to addition of binding partner and ligands; separation of bound from free ligand (by gel filtration) was performed exactly as described in the thermostability assay protocol (below).

Thermostability measurement of $\beta_1AR_{\Delta NC}$–mini-Gs complexes

Thermostability assays were performed using a modified version of previously described methods (Lebon *et al.*, 2011a; Serrano-Vega *et al.*, 2008). Insect cell membranes containing $\beta_1AR^{\Delta NC}$ were resuspended in assay buffer (25 mM HEPES pH 7.5, 400 mM NaCl,

1 mM $MgCl_2$, 1 mM ascorbate, 0.1% BSA, 0.004% bacitracin). The sample was aliquoted and binding partner (25 μM final concentration), ^{3}H-norepinephrine (200 nM final concentration) and apyrase (0.1 U/ml final concentration) were added. Norepinephrine was added to the negative control (200 μM final concentration). Samples were incubated at 4°C for 1 h, before solubilisation with detergent for 1 h on ice. The detergents dodecyl maltoside (DDM), decyl maltoside (DM), nonyl glucoside (NG) or octyl glucoside (OG) were used at final concentrations of 0.1, 0.13, 0.3 or 0.8%, respectively. Samples were heated to different temperatures (between 4 and 50°C) for exactly 30 min, followed by quenching on ice for 30 min. Samples were separated by gel filtration through Toyopearl HW-40F resin packed in a 96-well filter plate (Merck Millipore). Radioactivity was quantified by scintillation counting and apparent melting temperature (T_m) values were determined using GraphPad Prism version 5.0.

Thermostability measurement of GDP-bound mini-G_s mutants by differential scanning fluorimetry

Differential scanning fluorimetry (DSF) was performed essentially as described previously (Niesen *et al.*, 2007). Mini-G_s mutants (30 μg) were diluted with assay buffer (10 mM HEPES pH 7.5, 100 mM NaCl, 1 mM $MgCl_2$, 1 mM GDP, 2 mM DTT). SYPRO-orange was added to give a final concentration of ×2. Thermostability measurements were performed using a Rotor-Gene Q (Qiagen). Samples were equilibrated for 90 s at 25°C before ramping from 25 to 99°C at 4 s/°C. The apparent melting temperature (T_m), corresponding to the inflection point of the curve, was derived from analysis using the Rotor-Gene Q software.

Gel filtration analysis of mini G protein complexes

The mini-G_s–βγ complex was prepared using mini-G_s399, a construct in which the N-terminal residues 6–25 were replaced and the L272D mutation was reversed (Supplementary Table SIII). Purified mini-G_s399 was mixed with non-lipidated $G\beta_1\gamma_2$ dimer in an equimolar ratio and incubated on ice for 4 h. The sample was loaded onto a Superdex-200 10/300 gel filtration column (GE healthcare), equilibrated with gel filtration buffer (10 mM HEPES pH 7.5, 100 mM NaCl, 1 mM $MgCl_2$, 1 μM GDP, 0.1 mM TCEP).

The β_1AR–mini-G_s complex was prepared using $\beta_1AR^{\Delta NC}$ purified in lauryl maltose neopentyl glycol (LMNG) detergent. Purified $\beta_1AR^{\Delta NC}$ was mixed with a 1.2-fold molar excess of mini-G_s393 and incubated on ice for 4 h. The sample was loaded onto a Superdex-200 10/300 gel filtration column, equilibrated with gel filtration buffer (10 mM HEPES pH 7.5, 100 mM NaCl, 1 mM $MgCl_2$, 1 μM ascorbic acid, 1 μM isoprenaline, 0.002% LMNG). Peak fractions were analysed by SDS-PAGE on a 4–20% Tris-glycine gel (Thermo Fisher).

The gel filtration column was calibrated using molecular weight standards (Sigma), and the apparent molecular weight of samples was calculated using the calibration curve shown in Supplementary Fig. S9.

Statistical analysis

Unpaired, two-tailed *t*-tests were used to compare two data sets, and *P* values are quoted in the text.

Results

Strategy to develop a minimal G protein

The aim of this work was to isolate the minimum component of G_s that could be used to crystallise native-like GPCR–G protein complexes. The molecular weight of G_s is 90 kDa, however, the β_2AR–G_s complex (Rasmussen *et al.*, 2011b) revealed that more than 97% of direct contacts between the G protein and receptor are mediated by the 27 kDa GαGTPase domain (Fig. 1a). We hypothesised that this domain would be sufficient to stabilise GPCRs in their fully active state, i.e. the conformation adopted by β_2AR in the β_2AR–G_s complex (Rasmussen *et al.*, 2011b), and it was therefore used as the starting point to engineer a minimal G protein (mini-G_s; Fig. 1b).

Three binding partners were used as controls during this work: Nb80, a nanobody that binds to β_2AR and induces a comparable shift in agonist binding affinity to heterotrimeric G_s (Rasmussen *et al.*, 2011a); soluble heterotrimeric G_s that was mutated to remove all potential lipidation sites, referred to herein as G_s (Supplementary Table SI); and Nb35, a nanobody that stabilises G_s in its GPCR-bound conformation (Westfield *et al.*, 2011). G_s was either used alone (referred to as G_s) or in the presence of Nb35 (referred to as G_s–Nb35). As active state structures of β_2AR bound to either Nb80 or G_s–Nb35 have been determined (Rasmussen *et al.*, 2011a, 2011b), the stability and pharmacological activity of an engineered mini-G_s should, at a minimum, reflect the analogous properties of these binding partners.

The β_1-adrenergic receptor (β_1AR) was used as a model GPCR in the development of mini-G_s. Both β_1AR and β_2AR are able to bind G_s and Nb80 and exhibit a significant increase in agonist binding affinity. Either receptor could have been used for the development of mini-G_s, but because our laboratory has developed a large number of thermostabilised β_1AR variants (Miller and Tate, 2011; Serrano-Vega *et al.*, 2008), we chose to work with β_1AR. We did not use the adenosine A_{2A} receptor for the development of mini-G_s, because

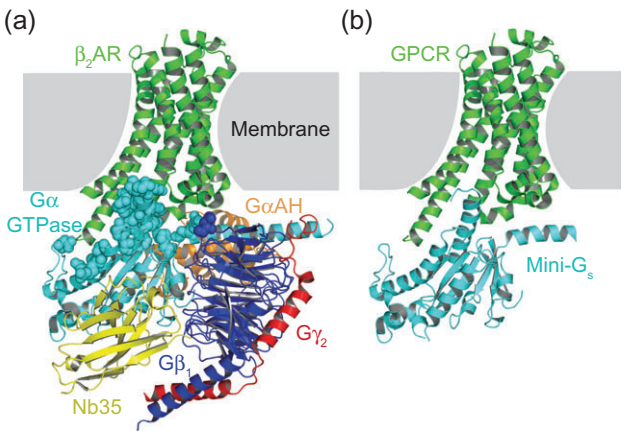

Fig. 1 Design of a minimal G protein. (**a**) Crystal structure of the β_2AR–G_s complex (PDB code 3SN6; Rasmussen *et al.*, 2011b). The intracellular component of this complex, which is composed of $G\alpha_s$, $G\beta_1$, $G\gamma_2$ and Nb35, totals over 100 kDa in molecular weight. However, over 97% of direct contacts (3.9 Å cut-off) between β_2AR and G_s are formed by the GαGTPase domain (cyan). Residues from G_s that form contacts with β_2AR are shown as spheres. (**b**) Model of the proposed complex between a GPCR and mini-G_s (isolated GαGTPase domain). The intracellular component of this complex is a single protein with a molecular weight of approximately 27 kDa. Figures were prepared using PyMOL (The PyMOL Molecular Graphics System, Version 1.7.4 Schrödinger, LLC)

there is only a small increase in agonist affinity upon binding a G protein (Carpenter *et al.*, 2016).

To be most useful for the characterisation and structure determination of GPCRs in their active state, mini-G_s needed to fulfil a number of criteria. Mini-G_s should be stable enough in its basal conformation to allow high-yield expression and purification, promote the transition of β_1AR to the high-affinity agonist-bound state, and form a stable complex with detergent-solubilised β_1AR. The development of mini-G_s involved a number of key steps, some of which only became apparent as the work progressed: (i) development of a sensitive assay to detect G protein coupling to β_1AR; (ii) isolation of the GαGTPase domain (mini-G_s) and demonstration of binding to β_1AR; (iii) thermostabilisation of the β_1AR–mini-G_s complex in membranes; (iv) thermostabilisation of the β_1AR–mini-G_s complex in detergent; and (v) validation of the final mini-G_s construct. Details of each of these steps are given under the corresponding subheadings later.

Development of a sensitive assay to detect G protein coupling to β_1AR

A sensitive competition binding assay was developed that could detect the interaction of different binding partners with β_1AR, by measuring the affinity of agonist binding to the receptor. A heterologous competition format was used to determine the agonist binding affinity (K_i) of β_1AR by measuring binding of the antagonist ^{3}H-dihydroalprenolol (^{3}H-DHA; Supplementary Fig. S1) in the presence of increasing concentrations of the agonist isoprenaline. The concentration of binding proteins used in the assays was standardised to 25 μM, which was approximately 30-fold above the equilibrium dissociation constant (K_D) for Nb80 binding to β_1AR (Miller-Gallacher *et al.*, 2014). Initially, we used a truncated form of turkey β_1AR (Warne *et al.*, 2003), which was designated $\beta_1AR^{\Delta NC}$ (Supplementary Table SII). This construct did not contain any thermostabilising mutations, and behaved identically to full-length receptor in cell-signalling assays (Baker *et al.*, 2011), despite containing truncations of disordered regions in the N-terminus and C-terminus. The K_i for isoprenaline binding to $\beta_1AR^{\Delta NC}$ was 40 ± 0 nM in the absence of a binding partner, which shifted to 5.8 ± 0.8 nM, 17 ± 2 nM or 6.8 ± 0.6 nM in response to Nb80, G_s or G_s–Nb35, respectively (Supplementary Fig. S2). The shift in isoprenaline K_i upon G protein binding to $\beta_1AR^{\Delta NC}$ was relatively small, which was unsuitable for detecting potentially small changes elicited upon binding of unstable G protein derivatives during the development of mini-G_s. We therefore used a minimally thermostabilised β_1AR construct (β_1AR-84; Supplementary Table SII), which contained four mutations that increased the stability preferentially of the inactive state of the receptor (Miller-Gallacher *et al.*, 2014; Warne *et al.*, 2011), in addition to the truncations at the N-terminus and C-terminus. β_1AR-84 had a lower affinity for isoprenaline (K_i of 2.6 ± 0.3 μM) in its uncoupled state than $\beta_1AR^{\Delta NC}$, but showed a larger shift in agonist binding affinity when coupled to either Nb80, G_s or G_s–Nb35 (K_i of 28 ± 1 nM, 271 ± 54 nM or 16 ± 4 nM, respectively; Table I and Supplementary Fig. S2). The competition binding data fitted best to single-site binding parameters. Therefore, the partial shift in isoprenaline K_i observed for some binding partners most likely reflected incomplete stabilisation of the high-affinity agonist-bound state, rather than indicating partial coupling or mixed receptor populations. Although G_s was able to couple β_1AR, Nb35 was required to stabilise the G_s complex, resulting in β_1AR–G_s–Nb35 complexes with similar affinity for isoprenaline compared to the β_1AR–Nb80 complexes (Table I and Supplementary Fig. S2). The competition binding assay using β_1AR-84 showed a 162-fold increase in isoprenaline affinity upon G_s–Nb35 coupling to the receptor, which was far larger than the 6-fold shift in affinity induced by G_s–Nb35 binding to $\beta_1AR^{\Delta NC}$. We therefore used β_1AR-84 in all subsequent competition binding assays during the development of mini-G_s.

Isolation of the Gα_s GTPase domain and measuring binding to β_1AR-84

The GαGTPase domain from Gα_s had previously been expressed as an isolated protein, in order to determine its role in guanine nucleotide binding and hydrolysis (Markby *et al.*, 1993), but its ability to couple to GPCRs had never been investigated. We isolated the GTPase domain by replacing the sequence corresponding to GαAH with a short glycine linker (Supplementary Table SIII). This construct, mini-G_s77, expressed poorly in *E. coli* and could not be purified to homogeneity, indicating that it was very unstable. Nevertheless, a small amount of partially pure protein could be prepared (Supplementary Fig. S3), and was tested for its ability to couple β_1AR-84 (at 20°C) in either the presence or absence of G$\beta\gamma$–Nb35. No significant shift in the isoprenaline K_i of β_1AR-84 (2.6 ± 0.3 μM) was observed in the presence of mini-G_s77 (1.9 ± 0.2 μM; $P = 0.254$), but mini-G_s77–G$\beta\gamma$–Nb35 induced a large shift in isoprenaline affinity to 3.6 ± 0.8 nM ($P = 0.004$; Table I and Supplementary Fig. S2). Thus partially purified mini-G_s77 was functional, but the data also suggested that it was unable to couple β_1AR-84 in the absence of G$\beta\gamma$ when assayed at 20°C. In contrast, when the assay was performed at 4°C mini-G_s77 induced a significant shift in isoprenaline K_i from 2.1 ± 0.2 μM for uncoupled β_1AR-84 (at 4°C) to 99 ± 12 nM ($P < 0.001$; Table I and Supplementary Fig. S2). This demonstrated that the isolated GαGTPase domain (mini-G_s77) could couple to β_1AR-84 in the absence of G$\beta\gamma$, but suggested that the thermostability of the GαGTPase domain was a limiting factor in its ability to stabilise the high-affinity agonist-bound state of the receptor.

Thermostabilisation of the β_1AR–mini-G_s complex in membranes

Rational design mutagenesis was employed to thermostabilise mini-G_s in complex with membrane-embedded β_1AR. Mutations were designed based on structural alignments (Fig. 2a and Supplementary Fig. S4) between Gα_s (Sunahara *et al.*, 1997) and Arl2 (Hanzal-Bayer *et al.*, 2002); Arl2 is the small GTPase with the greatest structural similarity to Gα_s. This initial mutagenic screen primarily targeted regions of Gα_s that were close to the GαAH domain interface or that were known to be conformationally dynamic. Mutants were screened using the competition binding assay at both 4 and 20°C. Due to the low, and variable expression level of the mutants, it was not easy to standardise the concentration of mini-G_s mutants used in the assays. Therefore, the total mini-G_s purified from 1 L of *E. coli* culture was used per competition curve (Table I). Approximately 100 mutants were tested during this initial screen. Mutations that shifted the isoprenaline K_i of β_1AR-84 more than 2-fold compared to the parental mini-G_s construct (mini-G_s77) at either temperature were classed as positive. A total of 16 positive mutations, covering 12 unique positions were identified (Table I).

Some of the single mini-G_s mutants produced a near maximal shift in the agonist binding affinity of β_1AR-84 in the competition binding assay, therefore, mutation combinations could not be

Table I. β_1AR-84 competition binding data

Binding partner	Mutation	CGN code[a]	β_1AR-84 isoprenaline K_i (nM)		Effect on expression
			4°C	20°C	
None	n.a.[b]	n.a.	2100 ± 180 (n = 12)	2600 ± 270 (n = 15)	n.a.
Nb80	n.a.	n.a.	n.d.[c]	28 ± 1 (n = 2)	n.a.
G_s	n.a.	n.a.	420 ± 80 (n = 2)	271 ± 54 (n = 2)	n.a.
G_s–Nb35	n.a.	n.a.	n.d.	16 ± 4 (n = 3)	n.a.
Mini-G_s77	Parental	n.a.	99 ± 12 (n = 4)	1900 ± 230 (n = 3)	n.a.
	H41I	$41^{G.S1.2}$	32	390	=
	H41V	$41^{G.S1.2}$	51	490	=
	A48L	$48^{G.s1h1.2}$	43	170	=
	G49D	$49^{G.s1h1.3}$	25	280	=
	E50N	$50^{G.s1h1.4}$	37	720	=
	R201A	$201^{G.hfs2.2}$	31	1480	−
	G226A	$227^{G.s3h2.2}$	86	820	=
	227–230 sub[d]	$227^{G.s3h2.3}$	23	530	=
	E230A	$230^{G.H2.3}$	51	540	−
	A249D	$249^{G.S4.7}$	10	35	+
	A249E	$249^{G.S4.7}$	70	390	=
	S252D	$252^{G.s4h3.3}$	14	94	+
	S252E	$252^{G.s4h3.3}$	38	380	+
	255–264 del[e]	$254^{G.s4h3.5}$	21	20	+
	L272D	$272^{G.H3.8}$	7	310	=
	L272E	$272^{G.H3.8}$	28	750	=

Competition binding data showing the isoprenaline K_i of β_1AR-84 in the presence of different binding partners. Data are from a single experiment performed in duplicate unless otherwise stated; where two or more independent experiments were performed, data represent mean ± SEM, from the number (n) of independent experiments performed in duplicate. The effect of mutations on the expression level of mini-G_s was estimated from SDS-PAGE gels. Expression levels are described as being equal to (=), more than 2-fold lower than (−), or more than 2-fold higher than (+) the parental construct.

[a]Common Gα numbering (CGN) system (Flock *et al.*, 2015).

[b]Not applicable.

[c]Not determined.

[d]Substitution of switch II residues 227–230 with two glycine residues.

[e]Deletion of switch III residues 255–264.

reliably tested using this assay, as further small increases in agonist affinity would be difficult to accurately measure. Instead, the mutation combinations were tested in complex with detergent-solubilised $\beta_1AR^{\Delta NC}$ using a thermostability (T_m) assay (Table II). The agonist ^{3}H-norepinephrine (^{3}H-NE) was used in the T_m assay, however due to the high background signal associated with this ligand, a maximum concentration of 200 nM could be used. This was approximately equal to the K_i of uncoupled $\beta_1AR^{\Delta NC}$, but approximately 250-fold above the K_i of $\beta_1AR^{\Delta NC}$ complexed with Nb80 or G_s–Nb35 (Supplementary Fig. S5). Therefore, apparent T_m values quoted for uncoupled $\beta_1AR^{\Delta NC}$ are under non-saturated agonist conditions, but $\beta_1AR^{\Delta NC}$ complexes, which have higher agonist binding affinity, are under agonist-saturated conditions.

A new parental construct (mini-G_s161), was used to test combinations of the mutations; mini-G_s161 contained a larger deletion encompassing GαAH with a slightly longer linker than in mini-G_s77 (Supplementary Table SIII). The A249D mutant (mini-G_s162) produced the largest shift in the agonist binding affinity of membrane-embedded β_1AR-84 in the competition binding assay, however, in detergent the $\beta_1AR^{\Delta NC}$–mini-G_s162 complex had an apparent T_m of 25.1°C (Table II), which was lower than that of uncoupled of $\beta_1AR^{\Delta NC}$ (25.9°C). Addition of the switch III deletion, which induced the second largest shift in the agonist binding affinity of membrane-embedded β_1AR-84, to make a double mutant (mini-G_s164), increased the apparent T_m of the complex to 28.6°C (Table II). However, this was still lower than that of either $\beta_1AR^{\Delta NC}$–Nb80 or $\beta_1AR^{\Delta NC}$–G_s–Nb35, by 3.4 and 7.2°C, respectively (Table II). Addition of other mutations that were classed as positive in the competition binding assay failed to further increase the apparent T_m of the $\beta_1AR^{\Delta NC}$–mini-G_s complex (examples shown in Table II), indicating that the complex was particularly unstable in detergent. This was confirmed by the observation that mini-G_s mutants were unable to shift the agonist binding affinity of detergent-solubilised β_1AR-84 to the same degree as that of membrane-embedded β_1AR-84 in competition binding assays (results not shown). Despite the fact that they did not further stabilise the $\beta_1AR^{\Delta NC}$–mini-G_s complex in detergent, four additional mutations (G49D, E50N, S252D and L272D) were added to mini-G_s164 to produce the construct mini-G_s183 (Table II). These mutations were utilised because they all individually increased the isoprenaline K_i of membrane-embedded β_1AR-84 (Table I). They also increased the stability of the basal GDP-bound state mini-G_s183 by 6°C compared to mini-G_s164 (Table II and Supplementary Fig. S6), as assessed by differential scanning fluorimetry.

Five of the six mutations that were combined in mini-G_s183 were clustered around the nucleotide-binding pocket and phosphate-binding loop (P-loop; Fig. 2a). The A249D mutation was designed to interact with Lys293 and Ser251, in order to stabilise the base of the nucleotide-binding pocket. Deletion of switch III was intended to stabilise mini-G_s, by replacing this flexible loop with the defined secondary structure elements (α-helix, 3_{10}-helix and β-turn) found in Arl2 (Hanzal-Bayer *et al.*, 2002). The S252D mutation was also

Table II. $\beta 1AR_{\Delta NC}$ thermostability data

Binding partner	Mutation	CGN code[a]	Apparent T_m of $\beta_1AR^{\Delta NC}$ in DDM, measured by ^{3}H-NE binding (°C)	Stability of GDP-bound mini-G_s measured by DSF (°C)
None	n.a.[b]	n.a.	25.9 ± 0.0 (n = 3)	n.a.
Nb80	n.a.	n.a.	32.0 ± 0.0 (n = 3)	n.a.
G_s–Nb35	n.a.	n.a.	35.8 ± 0.1 (n = 3)	n.a.
$G\alpha_s$	n.a.	n.a.	n.d.[c]	50.1 ± 0.1 (n = 3)
Mini-G_s162	A249D		25.1 (n = 1)	60.6 ± 0.1 (n = 3)
Mini-G_s164	A249D, SIII[d]		28.6 (n = 1)	66.5 ± 0.0 (n = 3)
Mini-G_s165	A249D, S252D, SIII		28.5 ± 0.2 (n = 2)	68.7 ± 0.0 (n = 3)
Mini-G_s169	A249D, S252D, SIII, L272D		28.8 (n = 1)	67.1 ± 0.0 (n = 3)
Mini-G_s183	G49D, E50N, A249D, S252D, SIII, L272D		28.7 ± 0.2 (n = 4)	72.5 ± 0.0 (n = 3)
Mini-G_s199[e]	G49D, E50N, A249D, S252D, SIII, L272D		29.2 ± 0.2 (n = 17)	72.5 ± 0.0 (n = 3)
Mini-G_s254	Mini-G_s199 + M60A	$60^{G.H1.8}$	31.5 ± 0.3 (n = 5)	70.3 ± 0.0 (n = 3)
Mini-G_s350	Mini-G_s199 + L63Y	$63^{G.H1.11}$	30.9 ± 0.4 (n = 2)	70.7 ± 0.0 (n = 3)
Mini-G_s340	Mini-G_s199 + I372A	$372^{G.H5.4}$	34.0 (n = 1)	66.6 ± 0.1 (n = 3)
Mini-G_s303	Mini-G_s199 + V375I	$375^{G.H5.7}$	31.5 ± 0.6 (n = 3)	70.3 ± 0.0 (n = 3)
Mini-G_s352	Mini-G_s199 + L63Y, I372A		34.5 (n = 1)	64.7 ± 0.1 (n = 3)
Mini-G_s345	Mini-G_s199 + I372A, V375I		35.0 (n = 1)	65.4 ± 0.1 (n = 3)
Mini-G_s393[f]	Final mini-G_s construct		34.1 ± 0.5 (n = 3)	65.3 ± 0.0 (n = 3)

Thermostability data for either detergent-solubilised $\beta_1AR^{\Delta NC}$ complexes or mini-G_s mutants in the GDP-bound state. Apparent T_m values represent the mean ± SEM from the number (n) of independent experiments performed in duplicate. Some apparent T_m values were determined from a single experiment, with an assumed error of ±0.5°C. Apparent T_m values for mini-G_s in the GDP-bound state were determined by differential scanning fluorimetry (Supplementary Fig. S6).

[a]Common Gα numbering (CGN) system (Flock *et al.*, 2015).

[b]Not applicable.

[c]Not determined.

[d]Deletion of switch III residues 255–264 is referred to as SIII.

[e]Mini-G_s199 contains the same mutations as mini-G_s183, but has a redesigned linker region (Supplementary Table SIII), and was used as the parental construct for screening detergent-stabilising mutations.

[f]Mini-G_s393 contains the same mutations as mini-G_s345, but has an additional truncation of the N-terminus and redesigned linker region (Supplementary Table SIII), and was used as the starting construct for crystallisation trials.

designed to stabilise the region around switch III, through a potential interaction with Arg265. The G49D and E50N mutations, which are located in the P-loop, were designed to reduce flexibility and conformationally constrain this region, through potential interactions with Arg265 and Lys293, respectively. The sixth mutation (L272D) was designed to conformationally constrain switch II, through potential interactions with a cluster of charged and polar residues (227–233) within its N-terminal region (Fig. 2b).

Thermostabilisation of the $\beta_1AR_{\Delta NC}$–mini-G_s complex in detergent

The majority of mutations from the first mutagenic screen did not stabilise the β_1AR–mini-G_s complex in detergent. We hypothesised that this was because they did not specifically stabilise mini-G_s in it receptor-bound conformation, therefore, a second panel of approximately 150 mutants were designed with the intention of stabilising the receptor-bound conformation of mini-G_s. This mutagenic screen was based on the structure of the β_2AR–G_s complex (Rasmussen *et al.*, 2011b), and focused on regions of $G\alpha_s$ that undergo large conformational changes upon receptor binding. Many of the mutations tested during this second screen were destabilising to mini-G_s in its basal GDP-bound state, therefore they could not be tested individually (i.e. in the mini-G_s161 parental construct). Instead, they were added to mini-G_s199, which was identical to mini-G_s183, except that it contained a modified linker region (Supplementary Table SIII). This construct was very stable in its basal GDP-bound state (72.5°C) and could thus negate the destabilising effects of the additional mutations. Mini-G_s mutants were screened in complex with detergent-solubilised $\beta_1AR^{\Delta NC}$ using the ^{3}H-norepinephrine T_m assay. Four stabilising mutations were identified (Table II), the best of which (I372A) increased the apparent T_m of the complex from 29.2 to 34.0°C and it combined additively with V375I, to give an apparent T_m of 35.0°C. This was 3.0°C higher than the $\beta_1AR^{\Delta NC}$–Nb80 complex and only 0.8°C lower than the $\beta_1AR^{\Delta NC}$–G_s–Nb35 complex. The other mutations did not combine additively with I372A and V375I and were rejected (results not shown).

Both of the positive detergent-stabilising mutations were located within the α1 or α5 helices. Alignment of $G\alpha_s$ in its receptor-bound conformation (Rasmussen *et al.*, 2011b) with the GTP-bound structure (Fig. 2c; Sunahara *et al.*, 1997) identified an unfavourable steric clash across the α1–α5 helix interface, involving residues Met60, His64 (from the α1 helix) and Ile372 (from the α5 helix). This clash was predicted to prevent close packing of the C-terminal region of the α1 helix against the α5 helix and the core of the GαGTPase domain, thus exposing the core of the protein to the solvent. The I372A mutation was designed to eliminate this clash and facilitate better packing in this region. Similarly, the V375I mutation was designed to improve packing between the α5 helix and the core of the protein in its receptor-bound conformation (Fig. 2d).

Validation of mini-G_s

The detergent-stabilised construct (mini-G_s345) was modified for crystallographic applications by changing the linker and shortening

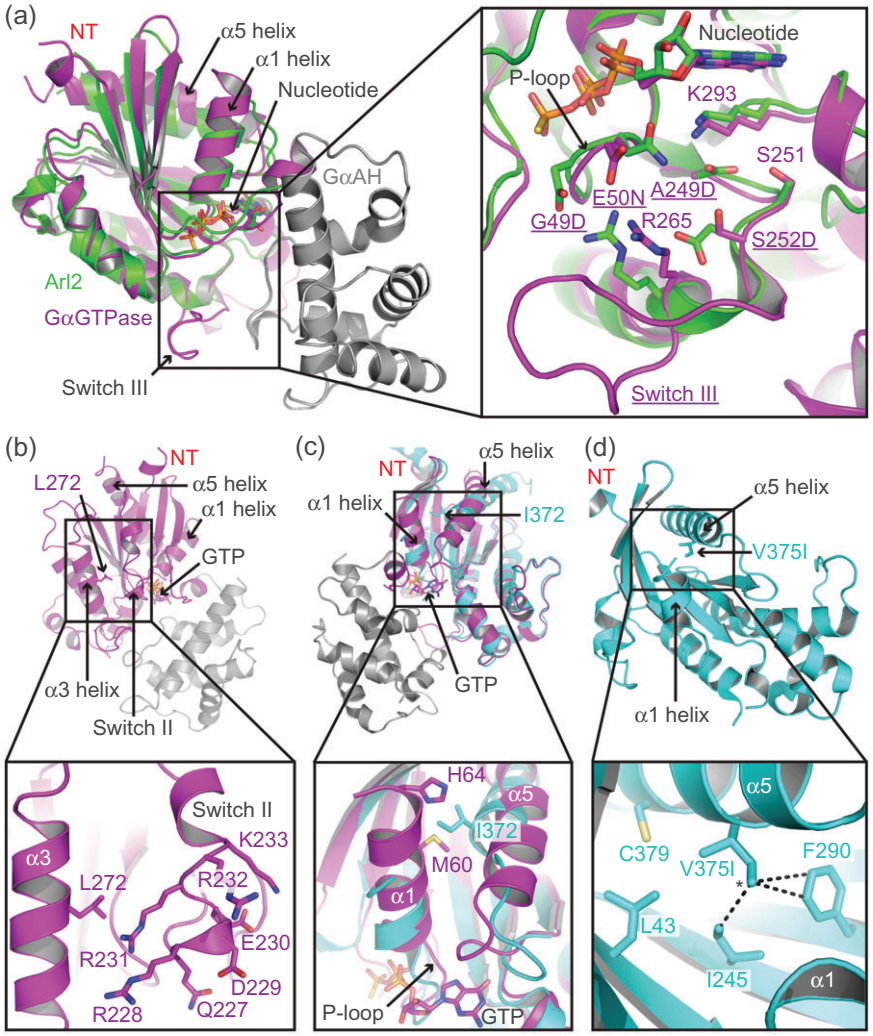

Fig. 2 Rational design of mutations to stabilise mini-G_s. (**a**) Structural alignment of $G\alpha_s$ (PDB code 1AZT; Sunahara *et al.*, 1997), coloured magenta and grey, and Arl2 (PDB code 1KSH; Hanzal-Bayer *et al.*, 2002), coloured green. The $G\alpha_s$ GTPase domain aligns to Arl2 with an RMSD of 1.9 Å, despite sharing sequence identity of only 25%, determined using the Dali server (Holm and Rosenstrom, 2010). See Supplementary Fig. S4 for a sequence alignment between $G\alpha_s$ and Arl-2. The inset shows an expanded view of mini-G_s residues (shown as sticks and underlined name) that were mutated (G49D, E50N, A249D, and S252D) to match the corresponding residue in Arl2. Residues with which the mutations potentially interact are shown as sticks. (**b**) Mutation of Leu272, which is located within the α3 helix of $G\alpha_s$ (PDB code 1AZT; Sunahara *et al.*, 1997), to aspartic acid allows potential interactions with a cluster of charged and polar residues (227–233) in the N-terminal region of switch II. (**c**) Alignment of $G\alpha_s$ in its GTP-bound conformation (PDB code 1AZT; Sunahara *et al.*, 1997), coloured magenta, and GPCR-bound conformation (PDB code 3SN6; Rasmussen *et al.*, 2011b), coloured cyan. In the GPCR-bound conformation Ile372 (α5 helix) sterically clashes with Met60 and His64 (α1 helix), preventing close packing of the α1 helix against the core of the GαGTPase domain. (**d**) The V375I mutation (modelled using PyMOL) was designed to increase hydrophobic contacts between the core of the GαGTPase domain and the α5 helix in its GPCR-bound conformation (PDB code 3SN6; Rasmussen *et al.*, 2011b). Residues that interact with Val375 are shown as sticks, additional contacts (less than 4.2 Å), which are predicted to be formed by the δ-carbon (*) of the isoleucine mutation are displayed as dashed lines.

the N-terminus (Supplementary Table SIII). The final stabilised construct, mini-G_s393 (Supplementary Fig. S7 and S8), was able to elicit an equal or greater shift in isoprenaline affinity compared to either Nb80 or G_s–Nb35 (Fig. 3a–c) whether the experiments were performed using membrane-embedded $\beta_1AR^{\Delta NC}$ (K_i of 4.1 ± 1.1 nM compared to 5.8 ± 0.8 nM and 6.8 ± 0.6 nM, respectively), membrane-embedded β_1AR-84 (K_i of 3.6 ± 0.0 nM compared to 28 ± 1 nM and 16 ± 4 nM, respectively) or detergent-solubilised β_1AR-84 (K_i of 4.7 ± 0.4 nM compared to 83 ± 2 nM and 23 ± 7 nM, respectively). Crucially, for the mini-G_s393 complex, high-affinity isoprenaline binding was maintained when β_1AR-84 was solubilised in detergent, and was 17-fold higher than that of the Nb80 complex and 5-fold higher than that of the G_s–Nb35 complex. Thus mini-G_s393 is an ideal protein for the formation of stable GPCR complexes in detergent solution.

The biochemical properties of mini-G_s393 also make it ideal for structural studies of GPCR complexes. Mini-G_s393 was readily purified to homogeneity with a yield of 100 mg of purified protein per litre of *E. coli* culture, and it could be concentrated to over 100 mg/ml (Supplementary Fig. S9). Analytical gel filtration showed that mini-G_s393 bound to purified $\beta_1AR^{\Delta NC}$ in LMNG (Fig. 3d and e), demonstrating that the complex could be purified in detergent. Recent innovations in electron cryo-microscopy (cryo-EM; Bai *et al.*, 2015) suggest that large GPCR–G protein complexes could be amenable for structure determination by single particle imaging. It is therefore useful to note that mini-G_s399, a construct in which the N-terminal

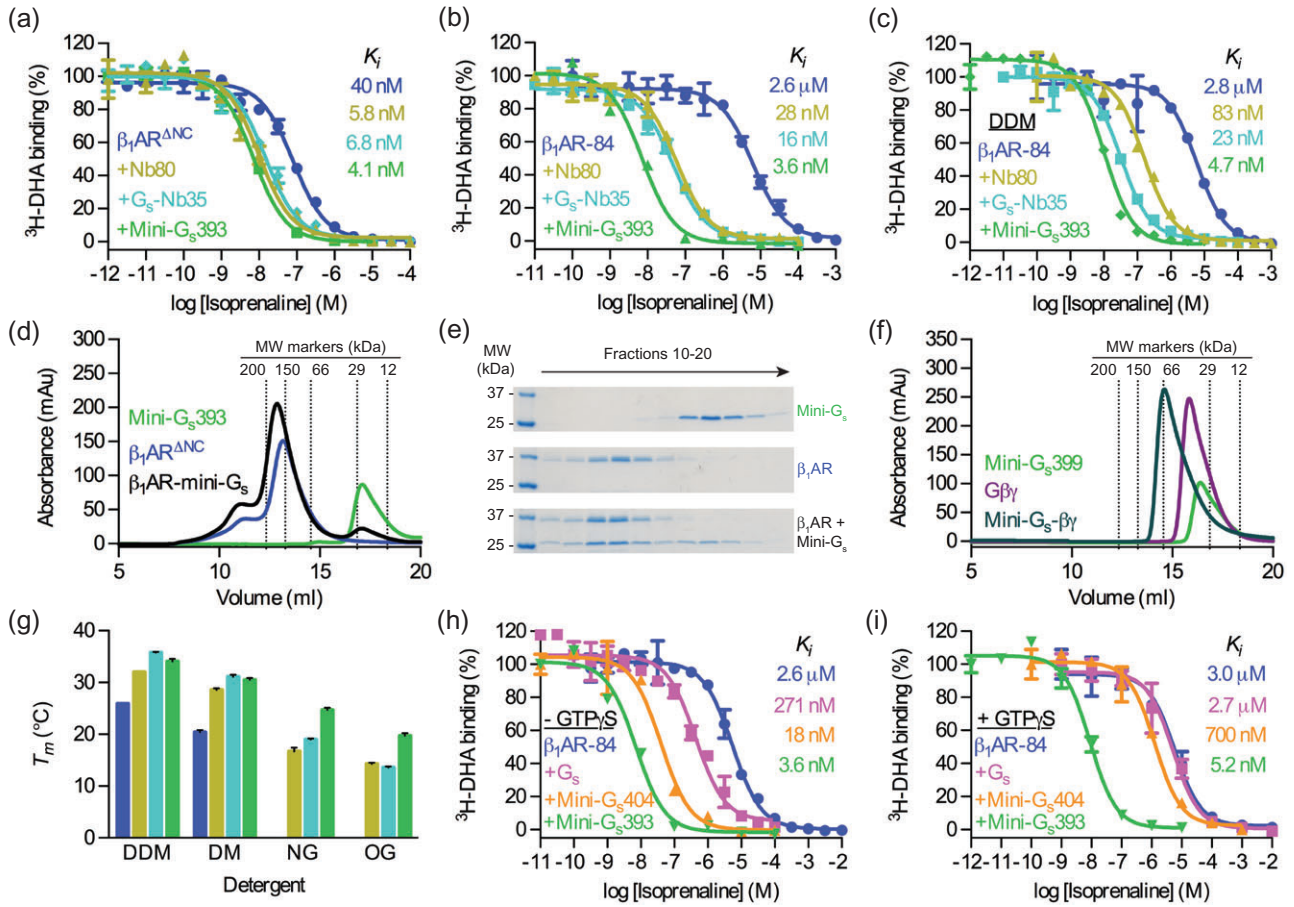

Fig. 3 Validation of mini-G_s (**a–c**) A competition binding assay was used to measure the change in affinity (K_i) of isoprenaline induced by Nb80, G_s–Nb35, or mini-G_s393 coupling to: (a) membrane-embedded $\beta_1AR^{\Delta NC}$, (**b**) membrane-embedded β_1AR-84 and (**c**) DDM-solubilised β_1AR-84. (**d**) Analytical gel filtration analysis of $\beta_1AR^{\Delta NC}$ binding to mini-G_s393. The apparent molecular weight of mini-G_s393 was 23 kDa (17.1 ml), which compares well with the theoretical value of 27 kDa. The apparent molecular weight of $\beta_1AR^{\Delta NC}$ was 139 kDa (13.2 ml), which is consistent with the 45 kDa receptor being associated with a large detergent micelle; the shoulder at 11 ml (> 300 kDa) probably represents aggregated receptor. A mixture of $\beta_1AR^{\Delta NC}$ and mini-G_s393 (1.2-fold molar excess) resolved as a predominant peak with an apparent molecular weight of 160 kDa (12.9 ml). The 21 kDa increase in the apparent molecular weight of the $\beta_1AR^{\Delta NC}$–mini-G_s393 complex compared to uncoupled $\beta_1AR^{\Delta NC}$ is consistent with mini-G_s393 binding with 1:1 stoichiometry. (**e**) SDS-PAGE analysis of the gel filtration eluate confirmed the presence of both $\beta_1AR^{\Delta NC}$ and mini-G_s393 in the peak fractions. (**f**) Analytical gel filtration analysis of Gβγ binding to mini-G_s399. The apparent molecular weights of mini-G_s399 (Supplementary Table SIII) and Gβγ were 32 kDa (16.4 ml) and 42 kDa (15.8 ml), respectively, which is in close agreement with the theoretical values of 29 kDa and 46 kDa, respectively. An equimolar mixture of mini-G_s399 and Gβγ resolved as a single peak with an apparent molecular weight of 73 kDa (14.6 ml). The 31 kDa increase in the apparent molecular weight of the mini-G_s399–Gβγ complex compared to Gβγ is consistent with mini-G_s399 binding with 1:1 stoichiometry. (**g**) Thermostability of detergent-solubilised $\beta_1AR^{\Delta NC}$ alone or in complex with Nb80, G_s–Nb35, or mini-G_s393, in different detergents (Supplementary Fig. S10). Uncoupled $\beta_1AR^{\Delta NC}$ did not survive solubilisation in NG or OG. Colours correspond to those used in (a). (**h–i**) GTP-mediated dissociation of β_1AR-84 complexes, measured by competition binding assay. The response in isoprenaline K_i induced by G_s, mini-G_s404 (Supplementary Table SIII), or mini-G_s393 coupling to β_1AR-84 was measured in the presence or absence of GTPγS (250 µM). (a–c,h,i) Data are representative of at least two independent experiments, each performed in duplicate, with error bars ± SEM. (g) Data represent mean ± SEM of at least two independent experiments, each performed in duplicate.

residues 6–25 were replaced and the L272D mutation was reverted to wild type (Supplementary Table SIII), retained its ability to form a heterotrimer with Gβγ (Fig. 3f). The main advantage of the mini-G_s399–Gβγ complex over heterotrimeric G_s, is that it lacks the GαAH domain, which is highly dynamic in the GPCR-bound conformation (Westfield *et al.*, 2011). Therefore GPCR complexes composed of mini-G_s399–Gβγ are predicted to be more conformationally homogenous than those involving heterotrimeric G_s, and thus better suited to cryo-EM applications.

Crystallisation of GPCRs often requires the use of short chain detergents, so the thermostability of the $\beta_1AR^{\Delta NC}$–mini-G_s393 complex was tested in four different detergents using the ^{3}H-norepinephrine T_m assay and compared to the analogous complexes with Nb80 and G_s–Nb35 (Fig. 3g and Supplementary Fig. S10). Under all conditions tested uncoupled $\beta_1AR^{\Delta NC}$ was significantly less stable than when bound to either mini-G_s393, Nb80 or G_s–Nb35. Similarly, $\beta_1AR^{\Delta NC}$ was always more stable bound to mini-G_s393 compared to Nb80. $\beta_1AR^{\Delta NC}$–mini-G_s393 complexes were also considerably more stable than $\beta_1AR^{\Delta NC}$–G_s–Nb35 complexes in short chain detergents, although the later was marginally more stable in DDM. The striking improvement in the thermostability by 5–8°C of the $\beta_1AR^{\Delta NC}$–mini-G_s393 complex in NG and OG in comparison to other complexes suggests it has significant advantages for the structure determination of receptors in the active state.

The nucleotide-binding properties of the mutants were not extensively studied in this work, but one interesting observation was that the β_1AR-84–mini-G_s393 complex was resistant to dissociation by physiological concentrations of GTP (Fig. 3h and i). GTPγS fully reversed the shift in K_i induced by G_s binding to β_1AR-84 from 271 ± 54 nM to 2.7 ± 0.1 μM. The shift in isoprenaline K_i induced by mini-G_s404 (an identical construct to mini-G_s393, except that the I372A and V375I mutations were reverted to wild type; Supplementary Table SIII) binding to β_1AR-84 was almost fully reversed by GTPγS (from 18 ± 2 nM to 700 ± 60 nM). However, there was no significant difference in the isoprenaline K_i of the β_1AR-84–mini-G_s393 complex in either the presence or absence of GTPγS (3.6 ± 0.0 nM compared to 5.2 ± 0.7 nM; $P = 0.137$). This unresponsiveness to GTPγS was caused by the I372A mutation (see Discussion), because mini-G_s391 (an identical construct to mini-G_s393, except that only the V375I mutation was reverted to wild type; Supplementary Table SIII), behaved in a similar fashion to mini-G_s393 (Supplementary Fig. S11). Unresponsiveness to GTP is a useful property that should allow the formation of stable GPCR–mini-G_s complexes *in vivo*, which may be a novel method to improve expression and purification of unstable GPCRs.

Discussion

Several novel approaches have been developed to stabilise and crystallise GPCRs in their active conformation, including complexation with G protein-derived peptides (Scheerer *et al.*, 2008), G protein-mimicking nanobodies (Huang *et al.*, 2015; Kruse *et al.*, 2013; Rasmussen *et al.*, 2011a; Ring *et al.*, 2013) and a nanobody-stabilised heterotrimeric G protein (Rasmussen *et al.*, 2011b). All of these complexes appear to stabilize the receptor in its active state, which is characterised by an outward movement of helix 6 and conserved conformational changes of residues within the core of the receptor, particularly $R^{3.50}$, $Y^{5.58}$ and $Y^{7.53}$ (Huang *et al.*, 2015). The β_2AR–G_s complex provided the first insight into the organisation of the native GPCR–G protein interface, which is something that other binding proteins cannot recreate, but frustratingly, complexes involving heterotrimeric G_s are also the most difficult to crystallise, due to their large size and dynamic nature. Therefore, we designed a minimal G protein that offers significant advantages to the crystallisation of native-like GPCR–G protein complexes, specifically mini-G_s is a small, soluble, highly expressed protein, which readily forms a detergent-stable complex with GPCRs.

Our lab has previously determined the structures of both β_1AR and the adenosine A_{2A} receptor (A_{2A}R) bound to agonists (Lebon *et al.*, 2011b; Warne *et al.*, 2011), and therefore crystallisation trials were conducted for both β_1AR and A_{2A}R in complex with mini-G_s, employing a parallel approach of lipidic cubic phase (LCP) and vapour diffusion. Crystals were obtained quickly for wild type A_{2A}R in complex with mini-G_s by vapour diffusion in the detergent octylthioglucoside (OTG), and we were able to solve the structure to 3.4 Å resolution (Carpenter *et al.*, 2016). β_1AR crystallisation trials are still at an early stage, and have not yet yielded crystals that diffract to sufficient resolution for structure determination. The molecular organisation of A_{2A}R–mini-G_s is remarkably similar to that of the β_2AR–G_s complex (Rasmussen *et al.*, 2011b), with A_{2A}R adopting a conformation that closely resembles G_s-bound β_2AR. In addition, mini-G_s bound to A_{2A}R is very similar to the analogous region in G_s bound to β_2AR (Rmsd 0.9 Å; Carpenter *et al.*, 2016). Thus mini G proteins are useful surrogates for heterotrimeric G proteins to stabilise and determine structures of GPCRs in their active conformation. However, it must be appreciated that GPCRs have not evolved to be stable in the activated state bound to a G protein, but instead have evolved to be unstable so that signalling lasts for short, defined, periods of time before being terminated. Therefore, additional approaches, such as thermostabilisation of the GPCR (Tate, 2012) bound to mini-G_s, may be required before the structures of many complexes can be determined. The high-level expression and stability of mini-G_s makes this a trivial undertaking compared to using the wild type heterotrimeric G protein. It is also important to note that further modifications of mini-G_s, such as deletions and mutations, may be required to facilitate crystallisation of different GPCRs. The crystal structure of the A_{2A}R–mini-G_s complex was solved using mini-G_s414, which is identical to mini-G_s393 except that it contains the additional mutation L63Y (Table II). Well diffracting crystals of the A_{2A}R–mini-G_s complex were grown using either mini-G_s393 or mini-G_s414, however, the A_{2A}R–mini-G_s414 complex produced a different crystal form that diffracted to slightly better resolution, and was thus used for structure determination. There was no discernible difference between these two complexes in either the competition binding assay or thermostability assay (results not shown), suggesting that the main effect of the L63Y mutation was on crystallogenesis.

The development of mini-G_s involved extensive screening to identify key deletions and point mutations that improved both the conformational homogeneity and thermostability of the β_1AR–mini-G_s complex (Fig. 4). Deletion of the GαAH domain, which is the most dynamic region of G_s in its GPCR-bound conformation, significantly reduced the conformational heterogeneity in the β_1AR–mini-G_s complex. This deletion also eliminated the requirement of Gβγ subunits for GPCR coupling, removing the need for exogenous components, such as Nb35, to stabilise the Gα–Gβγ interface. In the absence of Gβγ subunits the N-terminus of mini-G_s could be partially deleted, resulting in a more compact protein. The switch III

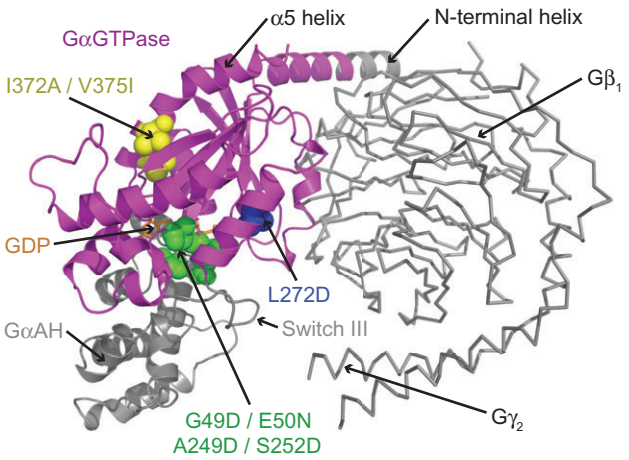

Fig. 4 A model of heterotrimeric G_s highlighting the region that corresponds to mini-G_s (magenta). The model of heterotrimeric G_s was constructed by superposition of the crystal structures of $G\alpha_s$ (PDB code 1AZT; Sunahara *et al.*, 1997) and heterotrimeric $G\alpha_{i/i1}$ (PDB code 1GOT; Lambright *et al.*, 1996). Residues that were mutated in mini-G_s (shown as spheres) were clustered in three regions of the protein: the nucleotide-binding pocket (green), switch II (blue), and the α5 helix (yellow). Regions of $G\alpha_s$ that were deleted in mini-G_s (GαAH, switch III and half of the N-terminal helix) are coloured grey. The Gβγ subunits, which are not required for mini-G_s coupling to GPCRs are shown as ribbons and coloured grey. GDP is shown as sticks and coloured orange.

deletion removed a dynamic region of mini-G_s, replacing it with defined secondary structure components, and resulted in a significant improvement in the thermostability of the complex. A total of seven point mutations were required to fully stabilise mini-G_s in complex with β_1AR (Fig. 4). Extensive mutagenic screens were employed that targeted most regions of mini-G_s, however, all of the mutations utilised in the final construct were clustered around three regions of the protein (nucleotide-binding pocket, switch II, and α5 helix). The G49D, E50N, A249D and S252D mutations were designed to stabilise the nucleotide-binding pocket and P-loop (Fig. 2a), and all of these mutations improved the thermostability of both the basal GDP-bound state of mini-G_s and the β_1AR–mini-G_s complex. The L272D mutation, which was located adjacent to switch II, was designed to conformationally constrain this flexible region (Fig. 2b), and resulted in improved thermostability of the β_1AR–mini-G_s complex. The I372A and V375I mutations, which were located in the α5 helix, were designed to improve packing between the core of protein and the α1 or α5 helices, respectively (Fig. 2c and d). These two mutations specifically improved the thermostability of the β_1AR–mini-G_s complex in detergent. None of these mutations were located within the receptor-binding site, ensuring that the native GPCR–G protein interface was maintained, and allowing mini-G_s to be co-crystallised with other G_s-coupled receptors. During the course of this work the I372A mutation was also independently reported to stabilise a complex between rhodopsin and the adenylate cyclase inhibiting G protein G_{i1} (Sun *et al.*, 2015).

The G protein engineering work has also provided insight into the mechanism of G protein activation. Binding of $G\alpha_s$ to β_2AR triggers displacement of the G protein α5 helix to a position that is predicted to sterically clash with the α1 helix. This unfavourable clash appears to prevent close packing of the C-terminal region of the α1 helix against the α5 helix and the core of the GTPase domain (Fig. 2c), and this region is indeed disordered in the β_2AR–G_s complex (Rasmussen *et al.*, 2011b). The α1 helix forms part of the nucleotide-binding pocket and directly connects to the P-loop (Fig. 2c), which is the main determinant of nucleotide binding affinity in G proteins (John *et al.*, 1990). Destabilisation of the α1 helix has previously been suggested to be a key event in receptor-mediated nucleotide exchange (Flock *et al.*, 2015; Kaya *et al.*, 2014; Sun *et al.*, 2015), however the mechanism of this destabilisation was unclear. Here, we identified a potential steric clash between Ile372 from the α5 helix and residues from the α1 helix (in particular Met60), which appears to play an important role in this nucleotide exchange. Mutation of Ile372 to alanine, which was predicted to eliminate the steric clash, was shown to inhibit GTP-mediated dissociation of the β_1AR–mini-G_s complex. These data indicate that, in G_s, Ile372 acts as a relay between the GPCR-binding site (α5 helix) and the key regions of the nucleotide-binding pocket (α1 helix and P-loop), allowing the receptor to allosterically destabilise the nucleotide-binding pocket and modulate nucleotide exchange. We suggest that the I372A mutation uncouples GPCR binding from occupancy of the nucleotide-binding pocket, a hypothesis that was supported by the presence of GDP in one of the two copies of mini-G_s in the asymmetric unit of the A_{2A}R–mini-G_s structure (Carpenter *et al.*, 2016).

Mini G proteins are novel tools that have many potential applications, including characterisation of receptor pharmacology in response to different classes of agonists (full, partial and weak), binding affinity and kinetic studies, thermostabilisation of GPCRs in their active conformation, drug discovery, and structure determination of native-like GPCR–G protein complexes. Furthermore, all of the mutations reported here are located within conserved regions of the Gα subunit. Therefore, the concept is potentially transferable to all classes of heterotrimeric G proteins, which would allow the production of a panel of mini G proteins capable of coupling any GPCR.

Supplementary data

Supplementary data are available at *PEDS* online.

Acknowledgement

We thank R. Nehmé, T. Warne and A.G.W. Leslie for comments on the article.

Funding

This work was funded by a grant from Heptares Therapeutics Ltd and core funding from the Medical Research Council [MRC U105197215].

References

Alexander,N.S., Preininger,A.M., Kaya,A.I., Stein,R.A., Hamm,H.E., and Meiler,J., (2014) *Nat. Struct. Mol. Biol.*, **21**, 56–63.

Bai,X.C., McMullan,G., and Scheres,S.H., (2015) *Trends Biochem. Sci.*, **40**, 49–57.

Baker,J.G., Proudman,R.G., and Tate,C.G., (2011) *Naunyn Schmiedebergs Arch. Pharmacol.*, **384**, 71–91.

Bornancin,F., Pfister,C., and Chabre,M., (1989) *Eur. J. Biochem.*, **184**, 687–698.

Carpenter,B., Nehme,R., Warne,T., Leslie,A.G., and Tate,C.G., (2016) *Nature*, **536**, 104–107.

Delean,A., Stadel,J.M., and Lefkowitz,R.J., (1980) *J. Biol. Chem.*, **255**, 7108–7117.

Dror,R.O., Mildorf,T.J., Hilger,D. *et al.* (2015) *Science*, **348**, 1361–1365.

Flock,T., Ravarani,C.N., Sun,D., Venkatakrishnan,A.J., Kayikci,M., Tate,C.G., Veprintsev,D.B., and Babu,M.M., (2015) *Nature*, **524**, 173–179.

Fung,B.K., Hurley,J.B., and Stryer,L., (1981) *Proc. Natl. Acad. Sci. USA*, **78**, 152–156.

Hamm,H.E., Deretic,D., Arendt,A., Hargrave,P.A., Koenig,B., and Hofmann, K.P., (1988) *Science*, **241**, 832–835.

Hanzal-Bayer,M., Renault,L., Roversi,P., Wittinghofer,A., and Hillig,R.C., (2002) *EMBO J.*, **21**, 2095–2106.

Herrmann,R., Heck,M., Henklein,P., Hofmann,K.P., and Ernst,O.P., (2006) *J. Biol. Chem.*, **281**, 30234–30241.

Higashijima,T., Ferguson,K.M., Sternweis,P.C., Smigel,M.D., and Gilman,A. G., (1987) *J. Biol. Chem.*, **262**, 762–766.

Holm,L. and Rosenstrom,P., (2010) *Nucleic Acids Res.*, **38**, W545–W549.

Huang,W., Manglik,A., Venkatakrishnan,A.J. *et al.* (2015) *Nature*, **524**, 315–321.

John,J., Sohmen,R., Feuerstein,J., Linke,R., Wittinghofer,A., and Goody,R.S., (1990) *Biochemistry*, **29**, 6058–6065.

Kaya,A.I., Lokits,A.D., Gilbert,J.A., Iverson,T.M., Meiler,J., and Hamm,H.E. , (2014) *J. Biol. Chem.*, **289**, 24475–24487.

Kruse,A.C., Ring,A.M., Manglik,A. *et al.* (2013) *Nature*, **504**, 101–106.

Kuhn,H., (1981) *Curr. Top. Membr. Trans.*, **15**, 171–201.

Lagerstrom,M.C. and Schioth,H.B., (2008) *Nat. Rev. Drug Discov.*, **7**, 339–357.

Lambright,D.G., Sondek,J., Bohm,A., Skiba,N.P., Hamm,H.E., and Sigler,P. B., (1996) *Nature*, **379**, 311–319.

Lebon,G., Bennett,K., Jazayeri,A., and Tate,C.G., (2011a) *J. Mol. Biol.*, **409**, 298–310.

Lebon,G., Warne,T., Edwards,P.C., Bennett,K., Langmead,C.J., Leslie,A.G., and Tate,C.G., (2011b) *Nature*, **474**, 521–525.

Markby,D.W., Onrust,R., and Bourne,H.R., (1993) *Science*, **262**, 1895–1901.

Miller,J.L., and Tate,C.G., (2011) *J. Mol. Biol.*, **413**, 628–638.

Miller-Gallacher,J.L., Nehme,R., Warne,T., Edwards,P.C., Schertler,G.F., Leslie,A.G., and Tate,C.G., (2014) *PLoS One*, **9**, e92727.
Niesen,F.H., Berglund,H., and Vedadi,M., (2007) *Nat. Protoc.*, **2**, 2212–2221.
Oldham,W.M., Van Eps,N., Preininger,A.M., Hubbell,W.L., and Hamm,H.E. , (2006) *Nat. Struct. Mol. Biol.*, **13**, 772–777.
Phillips,W.J., Wong,S.C., and Cerione,R.A., (1992) *J. Biol. Chem.*, **267**, 17040–17046.
Rasmussen,S.G., Choi,H.J., Fung,J.J. *et al.* (2011a) *Nature*, **469**, 175–180.
Rasmussen,S.G., DeVree,B.T., Zou,Y. *et al.* (2011b) *Nature*, **477**, 549–555.
Ring,A.M., Manglik,A., Kruse,A.C., Enos,M.D., Weis,W.I., Garcia,K.C., and Kobilka,B.K., (2013) *Nature*, **502**, 575–579.
Rosenbaum,D.M., Rasmussen,S.G., and Kobilka,B.K., (2009) *Nature*, **459**, 356–363.
Rosenbaum,D.M., Zhang,C., Lyons,J.A. *et al.* (2011) *Nature*, **469**, 236–240.
Scheerer,P., Park,J.H., Hildebrand,P.W., Kim,Y.J., Krauss,N., Choe,H.W., Hofmann,K.P., and Ernst,O.P., (2008) *Nature*, **455**, 497–502.
Serrano-Vega,M.J., Magnani,F., Shibata,Y., and Tate,C.G., (2008) *Proc. Natl. Acad. Sci. U S A*, **105**, 877–882.
Spiegel,A.M., Backlund, P.S., Jr, Butrynski,J.E., Jones,T.L., and Simonds,W. F., (1991) *Trends Biochem. Sci.*, **16**, 338–341.
Sprang,S.R., (1997) *Annu. Rev. Biochem.*, **66**, 639–678.
Sun,D., Flock,T., Deupi,X. *et al.* (2015) *Nat. Struct. Mol. Biol.*, **22**, 686–694.
Sunahara,R.K., Tesmer,J.J., Gilman,A.G., and Sprang,S.R., (1997) *Science*, **278**, 1943–1947.
Tate,C.G., (2012) *Trends Biochem. Sci.*, **37**, 343–352.
Van Eps,N., Preininger,A.M., Alexander,N., Kaya,A.I., Meier,S., Meiler,J., Hamm,H.E., and Hubbell,W.L., (2011) *Proc. Natl. Acad. Sci. U S A*, **108**, 9420–9424.
Vuong,T.M., Chabre,M., and Stryer,L., (1984) *Nature*, **311**, 659–661.
Warne,T., Chirnside,J., and Schertler,G.F., (2003) *Biochim. Biophys. Acta*, **1610**, 133–140.
Warne,T., Moukhametzianov,R., Baker,J.G., Nehme,R., Edwards,P.C., Leslie,A.G., Schertler,G.F., and Tate,C.G., (2011) *Nature*, **469**, 241–244.
Warne,T., Serrano-Vega,M.J., Tate,C.G., and Schertler,G.F., (2009) *Protein Expr. Purif.*, **65**, 204–213.
Westfield,G.H., Rasmussen,S.G., Su,M. *et al.* (2011) *Proc. Natl. Acad. Sci. U S A*, **108**, 16086–16091.
Xu,F., Wu,H., Katritch,V., Han,G.W., Jacobson,K.A., Gao,Z.G., Cherezov, V., and Stevens,R.C., (2011) *Science*, **332**, 322–327.